time accuracy of NPARC outflow boundary conditions for unsteady flow simulations is still an issue).

Figure 3 shows the pressure as a function of time at a point 5.0 in. upstream of the initial normal shock location. Results are shown for the fourth-order Runge–Kutta solver without smoothing, CFL = 0.9, and the pentadiagonal solver with CFL = 0.9, 1.8, and 4.4. Results obtained with the Runge–Kutta solver with smoothing and CFL = 0.9 and 4.4 are not shown in Fig. 3 since the residual smoothing caused the wave speed to be underpredicted by approximately 50% for both CFL = 0.9 and 4.4.

It is apparent from Fig. 3 that the Runge–Kutta solver without smoothing and CFL = 0.9 gives excellent agreement with the analytic result. The pentadiagonal solver gives reasonable agreement for CFL numbers up to 4.4. The error in the predicted arrival time for the normal shock is 0.6 ms (3.2%) with CFL = 0.9 and 2.2 ms (11.2%) with CFL = 4.4. Note, however, that the calculations with the pentadiagonal solver are significantly less expensive with the required computer time reduced to between 8 and 41% of the computer time required for the Runge–Kutta solver. Also note that the shape of the pressure profile is nearly the same regardless of the solver or CFL setting.

## Conclusions

The following conclusions are drawn from this study.

1) The standing wave flow proposed for evaluation of numerical accuracy issues associated with inlet unstart simulations is similar to the unsteady flow in the throat of an inlet in an inlet unstart simulation. The disturbance strength in the standing wave analysis can be selected so that the velocity of the normal shock relative to a fixed frame of reference is almost identical to the velocity of the normal shock near the throat of an inlet during an inlet unstart. Since the shock propagation velocity for a shock tube is several orders of magnitude higher than that in the throat of an inlet for even a weak shock, the standing wave analysis is better for evaluating unsteady flow solver, grid, and time step options for inlet unstart simulations.

2) Residual smoothing causes the wave speed to be underpredicted (by about 50% for the conditions analyzed).

3) For the disturbance magnitudes anticipated for an HSCT inlet, the shape of the wave was preserved for all of the smoothing, solver, and CFL options investigated (i.e., fourth-order Runge–Kutta solver, pentadiagonal solver, and CFL = 0.9, 1.8, and 4.4).

4) Without residual smoothing, the fourth-order Runge–Kutta solver predicted a wave speed that was almost exactly equal to the analytic wave speed at a CFL = 0.9. For the same CFL number, the pentadiagonal solver was nearly as accurate. At CFL = 4.4, the wave speed predicted with the pentadiagonal solver was within 11.2% of the analytic. This would cause a lag in the wave arrival of about 2.2 ms for a typical inlet wind-tunnel model.

5) The CPU time required to achieve a solution with the pentadiagonal solver with CFL = 4.4 is only 8% of that required for Runge–Kutta solver with CFL = 0.9. A substantial saving in CPU time is possible if preliminary unsteady inlet simulations are done with the pentadiagonal solver with a CFL below 5. For more accuracy, the pentadiagonal solver can be used at a CFL less than 1. For best accuracy, the Runge–Kutta solver should be used at a CFL less than 1.

## References

[1]Sirbaugh, J. R., Cooper, G. K., Smith, C. F., Jones, R. R., Towne, C. E., and Power, G. D., "A Users Guide to NPARC," NASA Lewis Research Center and Arnold Engineering and Development Center, NPARC Alliance Rept., Arnold Air Station, TN, Nov. 1994.

[2]Mayer, D. W., and Paynter, G. C., "Boundary Conditions for Unsteady Supersonic Inlet Analyses," *AIAA Journal*, Vol. 32, No. 6, 1994, pp. 1200–1206.

[3]Chung, J., "Numerical Simulation of a Mixed Compression Supersonic Inlet Flow," AIAA Paper 94-0583, Jan. 1994.

[4]Shapiro, A. H., *The Dynamics and Thermodynamics of Compressible Fluid Flow*, Vol. 2, Ronald, New York, 1954, p. 1000.

# Unsteady Adaptive Wall Models for Wind-Tunnel Testing

Byeong-Hee Chang* and Bongzoo Sung†
*Korea Aerospace Research Institute, Taejon 305-333, Republic of Korea*
and
Keun-Shik Chang‡
*Korea Advanced Institute of Science and Technology, Taejon 305-701, Republic of Korea*

## Introduction

THE adaptive wall test section technique has a distinct advantage over other devices for reduction of wall interference in wind-tunnel testing. For two-dimensional steady flows, the wall adaptation strategy has been well established and, to some extent, has been effectively applied to three-dimensional steady flows. For unsteady flow testing, wall adaptation would be conceptually perfect if the streamline could be obtained for a dynamic model in free flight for which the wind-tunnel test section wall is to be instantaneously adjusted. However, this idea has never been realized in wind-tunnel experiments. Fixed steady wall adaptation with an interference correction has been used instead in earlier unsteady flow experiments.[1] Since this approach was originally developed for pure subsonic or supersonic flows, it has limitations in application to transonic flows that contain a large supersonic flow region. There have also been difficulties for flows oscillating with large amplitude.[1] Instead, slotted or perforated walls have been widely put into practice with a reduced model size to lower the wall interference. In this study relatively simple unsteady adaptive two-dimensional wall models that can be used for the supercritical as well as subcritical oscillatory flows are proposed.

## Numerical Procedure

The finite volume method[2] is used for the Euler equations to numerically assess performance of the wall models for the wind-tunnel test section mounted with an oscillating airfoil. A resultant system of ordinary differential equations is integrated by a four-stage Runge–Kutta time-stepping scheme. The cell area changes with time when the airfoil and/or the wind-tunnel wall are in unsteady motion.

Unsteady flow around an oscillating airfoil in the wind-tunnel test section is treated by a composite grid system sketched in Fig. 1. The grid includes the buffer region I between the fixed H-mesh block and the oscillatory wall, and the buffer region II between the fixed H-mesh block and the O-mesh block embedding the airfoil that is under rigid oscillatory motion with the airfoil. The computational cells in these buffer regions undergo temporal deformation prescribed by spatial interpolation between the adjacent time-dependent boundary positions.

## Unsteady Adaptive Wall Models

Three adaptive wall models based on the streamline concept can be considered when the airfoil is in harmonic oscillation, $\alpha = \alpha_m + \alpha_0 \sin \omega t$. Here, $\alpha$ is angle of attack and $\omega$ is oscillation frequency. The simplest model will be the conventional adaptive wall model we call steady-streamline fixed adaptive wall

Received Nov. 1, 1994; revision received Feb. 4, 1995; accepted for publication Feb. 20, 1995. 

*Senior Researcher, Aerodynamics Department, 59, Oun-dong, Yusung-gu.

†Head, Aerodynamics Department, 59, Oun-dong, Yusung-gu. Member AIAA.

‡Professor, Department of Aerospace Engineering, 371-1, Kusung-dong, Yusung-gu. Member AIAA.

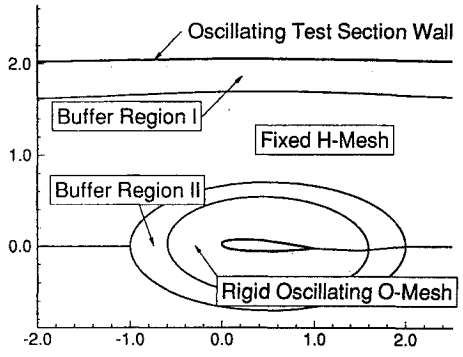


**Fig. 1 Multiblock grid for the oscillating airfoil.**

(SSFAW), which does not require time-dependent movement of the wall. Its wall shape coincides with the steady streamline induced by the stationary airfoil at the mean angle of attack $\alpha_m$. Because of its simplicity and capability of reasonable prediction, the SSFAW model has been widely used with unsteady correction for unsteady flow wind-tunnel testing.[1]

However, in reality the streamlines of unsteady flow vary with time. For the oscillatory airfoil, considering that the streamlines are also in harmonic motion, we can propose two additional unsteady adaptive wall models. The steady-streamline model-synchronized adaptive wall (SSMAW) is the wall oscillating between two limiting wall shapes in synchronization with the airfoil. The two limiting wall shapes here coincide with the steady streamlines induced by a stationary airfoil at the extreme angles of attack, $\alpha_m + \alpha_0$ and $\alpha_m - \alpha_0$. The other model we propose is the unsteady-streamline lift-synchronized adaptive wall (USLAW). The two oscillation limits of the test section wall are now patterned after the unsteady streamlines that could be obtained at the instants of maximum lift and minimum lift in an oscillation cycle. In other words, oscillation of the wall in this case is synchronized with the aerodynamic force instead of the airfoil motion.

The wall adjustment mechanism for the SSFAW model will be somewhat different from that of the steady flow testing model. The additional requirement for the SSMAW or USLAW model is the mechanism to drive the wall time dependently in a preprogrammed mode. This will not be technically difficult in view of modern computer-base control technology.

## Results and Discussion

We consider two existing AGARD test results[3] for the harmonically oscillating airfoil, NACA 0012, in free flight:

AGARD CT1

$$M_\infty = 0.6, \qquad \alpha_m = 2.89 \text{ deg}, \qquad \alpha_0 = 2.41 \text{ deg}$$

$$\kappa = 0.0808$$

AGARD CT5

$$M_\infty = 0.755, \qquad \alpha_m = 0.016 \text{ deg}, \qquad \alpha_0 = 2.51 \text{ deg}$$

$$\kappa = 0.0814$$

where $\kappa = \omega C/(2U_\infty)$ is the reduced frequency and $C$ denotes the airfoil chord. These unsteady flows with no tunnel wall are computed by the present multiblock, deforming and moving mesh approach. Its results are compared with a separate computation made with an airfoil and mesh oscillating as a rigid body for validation purposes. The two results turned out very close and showed the same trend as the experimental data of the AGARD tests.

One major concern in testing the oscillatory flow is the resonance in the test section. Fromme and Golberg[4] have shown, using the results of the Bland integral method, that there are resonance heights in the test section for the oscillating airfoil:

$$\frac{H}{C} = \frac{(2n-1)\pi}{4\kappa}\frac{\beta}{M_\infty}, \qquad \text{with } \beta = \sqrt{1 - M_\infty}, n = 1, 2, \ldots$$

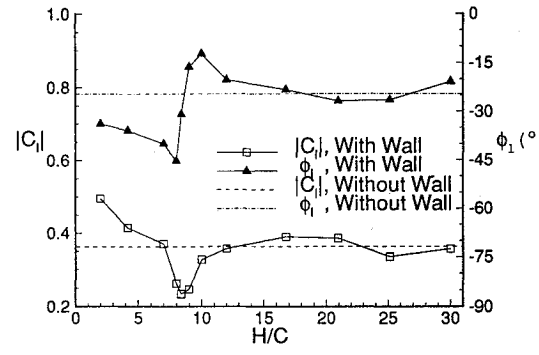


**Fig. 2 Amplitude and phase shift of the lift coefficient at resonance; AGARD CT5.**

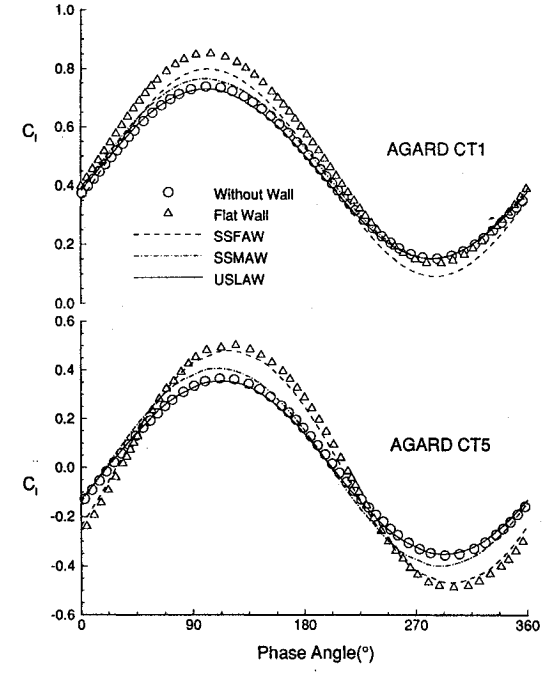


**Fig. 3 Performance of the adaptive wall models in transonic flows; $H/C = 2$.**

where $M_\infty$ is the freestream Mach number and $H$ is the distance to the wall from the oscillation center of the model.

Should there be resonance, the signal reflected from the test section wall would be canceled out by a succeeding disturbance radiated from the model surface. Consequently, measurement of the aerodynamic forces will vanish, and the phase shift angle will be abruptly changed to 90 deg.[1,4] In the present computation, similar phenomena can be observed in Fig. 2, where sudden change of $|C_l|$ and $\phi_l$ is apparent at $H/C = 8.38$. Here, the peak values of both amplitude and phase shift angle of the lift coefficient are attenuated much faster than the linearized inviscid theory has predicted.[4]

The computational results for the test case AGARD CT1 are represented in the upper curves of Fig. 3. They show that the three adaptive wall models, SSFAW, SSMAW, and USLAW, are all basically reasonable for the subcritical flow, with the three models having successively higher accuracy in eliminating the wall interference. However, the SSFAW model failed to reduce the wall interference sufficiently well for the supercritical flow or the AGARD CT5 case, as shown in the lower curves of Fig. 3. Here, the USLAW model exhibits the best performance, whereas SSMAW is superior to the SSFAW model whose wall is fixed with time.

The USLAW model remained best even near the resonance condition (not shown here), where the SSMAW model was evidently no longer accurate. The USLAW model, in this case, showed nearly correct amplitude with slight phase error. It should be noted, however, that testing near the resonance condition is the most severe case and

will be avoided in real wind-tunnel testing. When all of these factors are taken into account, one can conclude that the SSMAW model, which dispenses with the more complex unsteady streamlining procedure required by the USLAW model, can be generally a useful adaptive wall model.

## Conclusion

The existing SSFAW model is a reasonable means to reduce the wind-tunnel wall interference for the unsteady subcritical flow. However, the more sophisticated models such as SSMAW or USLAW are required for unsteady supercritical flows. The SSMAW model is an efficient wall model for both subcritical and supercritical flows provided we avoid testing near the wall resonance condition. The USLAW model produces the most accurate result, even near the resonance condition.

## References

[1]Forshing, H., and Voss, R., "Adaptation for Unsteady Flow," *Adaptive Wind Tunnel Walls: Technology & Applications*, AGARD-AR-269, April 1990, pp. 91–99.

[2]Venkatakrishnan, V., and Jameson, A., "Computation of Unsteady Transonic Flows by the Solution of Euler Equations," *AIAA Journal*, Vol. 26, No. 8, 1988, pp. 974–981.

[3]Landon, R. H., "NACA 0012 Oscillator, and Transient Pitching," *Compendium of Unsteady Aerodynamic Measurement*, AGARD-R-702, Aug. 1982, pp. 3.1–3.25.

[4]Fromme, J. A., and Golberg, M. A., "Aerodynamic Interference Effects on Oscillating Airfoils with Controls in Ventilated Wind Tunnels," *AIAA Journal*, Vol. 18, No. 4, 1980, pp. 417–426.

# Shock Oscillation in a Two-Dimensional, Flexible-Wall Nozzle

Shen-Min Liang,* Chou-Jiu Tsai,† and Fan-Ming Yu‡
*National Cheng Kung University,*
*Tainan 701, Taiwan, Republic of China*

## Introduction

FLUID/STRUCTURE interaction problems are of great interest to aeronautical engineers, since some components of modern aircraft tend to be flexible to achieve high performance. In this Note, the interaction problem caused by inviscid transonic flow in a two-dimensional, convergent-divergent nozzle with flexible walls is considered.

Felker[1] studied the static aeroelastic problem by means of a direct method that solved the fully coupled discretized fluid dynamic and structural equations to obtain the equilibrium solution. His computed solution of wall pressure ahead of the throat agreed reasonably well with the test data of Mason et al.[2] But Felker's solution deviated from the test data downstream of the throat. Therefore, the objective of this paper is twofold. The first is to obtain a reasonably accurate (equilibrium) solution by establishing a proper spring model for representing the wall flexibility. Felker used a simple spring model in which the wall deformation was assumed to be linearly related to the difference between the local internal wall pressure and the ambient static pressure. The deformed wall shape was represented by a set of discrete displacements at selected nodes. The elastic spring constant $k$ was assumed to be constant at each node. To achieve good accuracy, however, it is desirable to use a grid with grid points clustered near the throat. With Felker's spring model the nozzle wall may be too stiff at the throat region. To avoid this deficiency, the wall stiffness at each node is modified (described later) so that a more uniform wall elasticity is assured.

The second objective is to numerically investigate the transonic flow with shock oscillation caused by a downstream pressure fluctuation. Thus, the paper is an extension of our past research interest which was related to unsteady transonic flow with shock waves in a convergent-divergent channel with rigid walls.[3] The numerical simulation has been widely used for other aeroelastic problems.[4] The successful simulation of the two-dimensional problem is a stepping stone for studying three-dimensional aeroelastic nozzle problems.

## Mathematical Formulation

### Governing Equations

Without consideration of fluid flow viscosity and heat flux at the nozzle wall, the equations governing the nozzle flow with flexible walls are the time-dependent Euler equations.

### Model of Wall Flexibility

The wall flexibility is represented by the discrete spring model described subsequently. The discrete displacement $s$ at a selected node is assumed to be linearly related to the difference between the local internal wall pressure and the ambient static pressure. Unlike Felker's spring model, the elastic spring constant at node $i$, denoted by $k_i$, is set to be a constant $\bar{k}$ multiplied by a factor $w_i (<1)$ which is defined to be the ratio of the average of two adjacent element lengths, from point $(x_i, y_i)$ to points $(x_{i-1}, y_{i-1})$ and $(x_{i+1}, y_{i+1})$ on the wall, to the total length of the nozzle wall. If $w_i$ is set to be unity, the present spring model is reduced to Felker's model. The constant $\bar{k}$ is chosen such that the computed wall pressure matches the experimental data at some point.

## Numerical Procedure

### Discretization

The time-dependent Euler equations are discretized by a finite-volume approach associated with an improved implicit total-variation-diminishing (TVD) scheme of second order in time and space for unsteady flow calculation.[5] The present TVD scheme is basically the implicit TVD scheme of Yee and Harten[6] with an improved flux limiter.[5] The improved flux limiter allows the use of a larger Courant number for convergence. The discretized equations are solved with an approximate factorization of Beam and Warming[7] for computational efficiency.

### Boundary Conditions

*Flexible Wall*

Since the nozzle wall is flexible, the wall surface can move outward or inward. Let $(\dot{x}_i, \dot{y}_i)$ be the wall velocity at node $i$ at time $t$ and $s_i$ the wall displacement at node $i$ from time $t$ to time $t + \Delta t$. The wall velocity $(\dot{x}_i, \dot{y}_i)$ is determined by

$$\dot{x}_i = -\frac{s_i}{\Delta t}\frac{\Delta y_i}{d_i} \qquad \dot{y}_i = \frac{s_i}{\Delta t}\frac{\Delta x_i}{d_i}$$

where $(\Delta x_i, \Delta y_i)$ are defined as one-half of the coordinate differences between point $(x_{i+1}, y_{i+1})$ and point $(x_{i-1}, y_{i-1})$ on the wall; i.e.,

$$\Delta x_i = \frac{x_{i+1} - x_i}{2} + \frac{x_i - x_{i-1}}{2} = \frac{x_{i+1} - x_{i-1}}{2}$$

$$\Delta y_i = \frac{y_{i+1} - y_i}{2} + \frac{y_i - y_{i-1}}{2} = \frac{y_{i+1} - y_{i-1}}{2}$$

Also $d_i = \sqrt{\Delta x_i^2 + \Delta y_i^2}$ is the length of line segment formed by $(\Delta x_i, \Delta y_i)$; in other words, the line length $d_i$ is assigned to node $i$. The boundary condition on the wall is the condition of no normal flux across the wall (called the slip condition). Thus, the normal fluid velocity $V_n$ on the wall relative to the wall velocity must be zero, i.e.,

$$V_{ni} = 0$$

Received Oct. 31, 1994; revision received March 23, 1995; accepted for publication March 23, 1995. 

*Professor, Institute of Aeronautics and Astronautics. Member AIAA.

†Graduate Student, Institute of Aeronautics and Astronautics; currently Associate Professor, National Tainan Teachers College, Tainan 701, Taiwan, Republic of China.

‡Associate Professor, Institute of Aeronautics and Astronautics. Member AIAA.